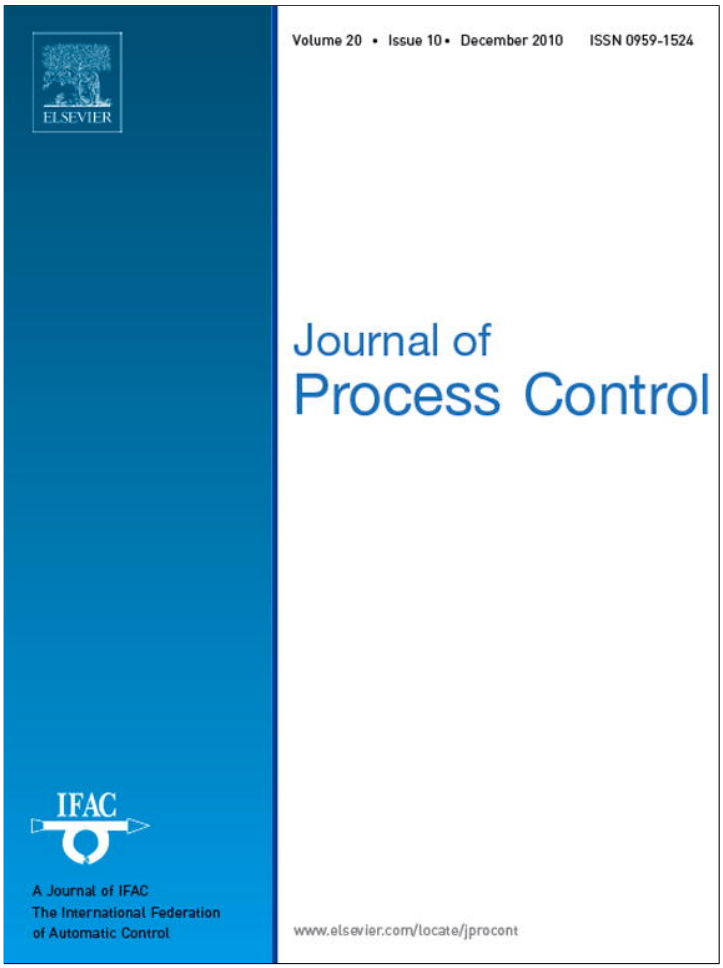

Journal of Process Control 20 (2010) 1261–1269

Contents lists available at ScienceDirect

Journal of Process Control

journal homepage: www.elsevier.com/locate/jprocont

# Minimizing energy consumption in reverse osmosis membrane desalination using optimization-based control

Alex R. Bartman [a], Aihua Zhu [a], Panagiotis D. Christofides [a,b,*], Yoram Cohen [a]

[a] Department of Chemical and Biomolecular Engineering, University of California, Los Angeles, CA 90095, USA
[b] Department of Electrical Engineering, University of California, Los Angeles, CA 90095, USA

ARTICLE INFO

*Article history:*
Received 18 May 2010
Received in revised form 16 August 2010
Accepted 24 September 2010

*Keywords:*
Reverse osmosis desalination
Energy optimization
Feedback control
Process control
Specific energy consumption

ABSTRACT

This work focuses on the design and implementation of an optimization-based control system on an experimental reverse osmosis (RO) membrane water desalination process in order to facilitate system operation at energy optimal conditions. A nonlinear model for the RO process is derived using first principles and the model parameters are computed from experimental data. This model is combined with appropriate equations for reverse osmosis system energy analysis to form the basis for the design of a nonlinear optimization-based control system. The proposed control system is implemented on UCLA's experimental RO desalination system and its energy optimization capabilities are evaluated.



## 1. Introduction

In recent years, the interest in the use of reverse osmosis membrane desalination has increased due to the energy efficiency and versatility of this process relative to other water desalination technologies [1]. Water shortages in various areas of the world have necessitated further development of the reverse osmosis desalination process in order to provide clean drinking water to the people in these regions. When operating a reverse osmosis desalination process, it is imperative that the system conditions are monitored and maintained at appropriate set-points in order to produce the required amount of clean, potable water while preventing system damage. Furthermore, with the rising cost of energy, it is also desired to find operating methods to reduce the energy consumption of reverse osmosis desalination processes in the presence of feed water variability. This task requires the development and implementation of effective feedback control strategies.

Traditionally, classical (i.e., proportional–integral (PI) or proportional–integral–derivative (PID)) control algorithms have been used to regulate process flow rates and adjust the system pressure in order to achieve a desired rate of clean water production [2]. In addition to classical control schemes, nonlinear model-based geometric control strategies have been developed to minimize the effects of varying feed water quality and also to account and correct for various faults that may present themselves during the operation of a reverse osmosis desalination process [3,4]. Control methods using model-predictive control (MPC) and Lyapunov-based control have also been evaluated using computer simulations [4–8]. With respect to results in the broad area of optimization-based control, the reader may refer to the following papers for results on real-time optimization (e.g., [9]), self-optimizing control (e.g., [10]), and extremum-seeking control (e.g., [11]). Reverse osmosis system analysis using linear models and data-based models using step-tests to create approximate linear models have also been demonstrated [12]. Other control methods have also been evaluated in the context of RO system integration with renewable energy sources [13,14]. While the aforementioned control strategies are able to maintain a constant permeate production rate and deal with feed water variability, they do not directly optimize energy usage by the reverse osmosis process.

Recently, extensive effort has been devoted to the issue of reverse osmosis system energy consumption. In a typical seawater RO system, the cost of energy can approach 45% of the total permeate production cost due to the fact that the system operation can require very high feed pressures (around 1000 psi) in order to achieve a desired permeate production rate [15–17]. Several efforts have been made in order to decrease the energy required by a reverse osmosis desalination system; these include work in increasing membrane permeability leading to lower required transmembrane pressure [18,19], optimization of RO module and

* Corresponding author at: Department of Chemical and Biomolecular Engineering, University of California, 5531 Boelter Hall, Los Angeles, CA 90095, USA.
Tel: +1 310 794 1015; fax: +1 310 206 4107.
*E-mail address:* pdc@seas.ucla.edu (P.D. Christofides).

0959-1524/$ – see front matter © 2010 Elsevier Ltd. All rights reserved.
doi:10.1016/j.jprocont.2010.09.004

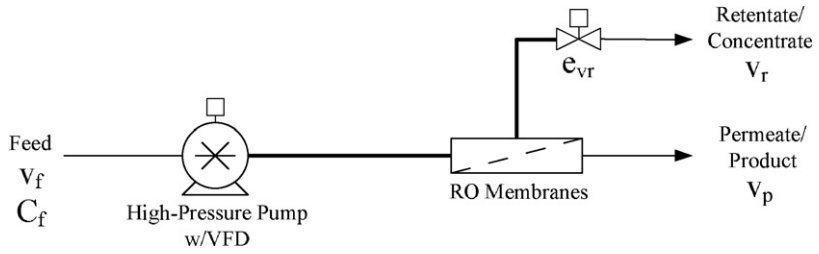


**Fig. 1.** Simplified reverse osmosis (RO) membrane desalination system used in model development.

system configuration [20,21], and also the use of energy recovery devices. In the area of energy optimization, it has been recently shown that the specific energy consumption, or SEC (energy cost per volume of permeate water produced), is useful as a metric to quantify reverse osmosis desalination system energy usage. Within the SEC framework, the issues of unit cost optimization with respect to water recovery, energy recovery, system efficiency, feed/permeate flow rate, membrane module topology [21–23], and optimization of the transmembrane pressure subject to feed salinity fluctuations have been studied [24]. However, no experimental verification of the theoretically computed energy optimal operating points was done in our previous work [21–24].

In this work, feedback control is integrated with an SEC-based energy optimization algorithm in order to maintain RO system operation at energy-optimal conditions. First, a reverse osmosis desalination system model is derived from mass and energy balances. Next, the system model is used in conjunction with the system energy usage analysis equations developed in [21,24] to design an energy optimization-based controller. This controller uses multiple system variables and a user defined permeate production rate to calculate the optimal operating set-points that minimize the specific energy consumption of the reverse osmosis desalination system and satisfy the process and control system constraints. The optimization-based control system is implemented in a multi-tiered fashion on UCLA's experimental RO system and the data from the experiments are shown to correspond closely to the theoretically predicted energy consumption curves. This work is clearly distinct from [3] where the emphasis was on nonlinear dynamic modeling of the experimental RO system and on nonlinear multivariable control.

## 2. RO system model

In order to utilize optimization-based control algorithms, a reverse osmosis system model must be derived. A simple RO process is used as the basis for the model derivation, as seen in Fig. 1; this process captures the main characteristics of UCLA's experimental RO system. In this process, the feed water enters at atmospheric pressure and is pressurized by a high-pressure pump. The pressurized feed stream is fed to the reverse osmosis membrane module and is split into a clean water (permeate) stream, and a concentrated brine (retentate) stream. After the retentate stream exits the reverse osmosis module, it passes through an actuated retentate valve that can be used to adjust the retentate stream flow rate and the system pressure.

For the model RO process in Fig. 1, mass and energy balances are used to derive model equations for the retentate stream velocity and the system pressure. In the derivation, it is assumed that the water is incompressible, all components are operated on the same plane (i.e., potential energy terms due to gravity are neglected), and the density of the water is assumed to be constant. Owing to the fast dynamics of the process, the steady state representation of the model equations are used in the optimization algorithm in this work. Specifically, using a kinetic energy balance around the actuated retentate valve, the following steady state equation is obtained:

$$0 = \frac{A_p^2}{A_m K_m V}(v_f - v_r) + \frac{A_p}{\rho V}\Delta\pi - \frac{1}{2}\frac{A_p e_{vr} v_r^2}{V} \tag{1}$$

where $v_r$ is the retentate stream velocity, $A_p$ is the pipe cross-sectional area, $A_m$ is the active membrane surface area, $K_m$ is the overall mass transfer coefficient, $V$ is the system volume, $v_f$ is the feed stream velocity, $\rho$ is the fluid density, $\Delta\pi$ is the osmotic pressure difference across the surfaces of the membrane, and $e_{vr}$ is the retentate valve resistance. It is assumed that the equation for the relationship between osmotic pressure and concentration can be represented as:

$$\Delta\pi = f_{os} C_{feed} \frac{\ln(1/(1-Y))}{Y} \tag{2}$$

where $f_{os}$ is an empirically obtained constant ($f_{os} = 78.7$) [21], $C_{feed}$ is the total dissolved solids concentration of the feed solution, and $Y$ is the overall system recovery:

$$Y = \frac{Q_p}{Q_f} = \frac{Q_p}{Q_p + Q_r} = \frac{v_p}{v_p + v_r} \tag{3}$$

where $Q_p$ is the permeate stream flow rate, $v_p$ is the permeate stream velocity (this can also be represented by the mass balance, $v_p = v_f - v_r$), $Q_r$ is the retentate stream flow rate, and $Q_f$ is the feed stream flow rate. The osmotic pressure difference (Eq. (2)) is also utilized in the algebraic equation for system pressure, $P_{sys}$, which is derived from an overall system mass balance:

$$P_{sys} = \frac{\rho A_p}{A_m K_m}(v_f - v_r) + \Delta\pi \tag{4}$$

From Eq. (4), the permeate stream velocity ($v_p$) can be determined by:

$$v_p = \frac{A_m K_m}{\rho A_p}(P_{sys} - \Delta\pi) \tag{5}$$

Additional information regarding the model derivation can be found in [3]. The unknown system parameters ($K_m$, $V$) were calculated from experimental step-test data and the resulting parameter values can be found in Table 1. The other model parameters are known properties of the experimental system ($\rho$, $A_p$, $A_m$) and are also listed in Table 1. For the optimization calculations conducted in this work, velocity was given in terms of meters per second, pressures given in Pascal, and flow rates were utilized in the units of cubic meters per second.

**Table 1**
Process model parameters based on experimental system data.

| | |
|---|---|
| $\rho = 1007$ | kg/m$^3$ |
| $V = 0.6$ | m$^3$ |
| $A_p = 0.000127$ | m$^2$ |
| $A_m = 15.6$ | m$^2$ |
| $K_m = 9.7 \times 10^{-9}$ | s/m |

As mentioned above, the metric used to determine the energy usage of the reverse osmosis desalination system is the specific energy consumption, or SEC. The SEC is defined as [21]:

$$SEC = \frac{\Delta P}{Y} = \frac{P_{sys}}{Y} = \frac{P_{sys}Q_f}{Q_p} \tag{6}$$

where $\Delta P$ is the pressure generated by the high-pressure pump (equal to $P_{sys}$ in this work because it is assumed that the raw feed pressure is equal to atmospheric pressure) and $Y$ is the water recovery as defined in Eq. (3). The SEC can also be normalized with respect to the osmotic pressure of the feed ($\pi_0$) as follows:

$$SEC_{norm} = \frac{SEC}{\pi_0} \tag{7}$$

In this model formulation for the evaluation of system energy usage, it is assumed that the salt rejection of the membranes is equal to unity. In addition to the RO system model, it is also important to model the correlation between valve resistance and the valve setting as controlled in the experimental system. This correlation is instrumental in allowing the feedback controller to implement control actions on the experimental system; accomplished by translating the valve resistance into a valve position, which can then be applied to the actuated retentate valve. The correlation used in this work is similar to the correlation computed in [3]; the valve position ($O_p$) is related to the valve resistance by five logarithmic relations, each used in a different range of valve resistance values (or equivalently, a different range of valve positions). This increases the accuracy of the correlation in the work presented in [3] where only three logarithmic relations are used to fit the experimental valve data. The general form of the logarithmic relation can be represented by:

$$e_{vr} = \alpha \ln O_p + \beta \tag{8}$$

where the values for $\alpha$ and $\beta$ for each valve position range can be found in Table 2.

The correlations are shown along with the manufacturer's suggested valve curve in Fig. 2. It should be noted that the valve in these experiments is limited to 70% of its full range due to the fact that the 10-turn valve is actuated with a 7-turn motor.

**Table 2**
Logarithmic correlation parameters for conversion of valve position to valve resistance.

| Position range | $\alpha$ | $\beta$ |
|---|---|---|
| 0–0.7% | −512,287 | −167,284 |
| 0.7–1.4% | −12,425 | 11,043 |
| 1.4–7% | −2052 | 7434 |
| 7–49% | −1436 | 6092 |
| 49–70% | −265 | 1554 |

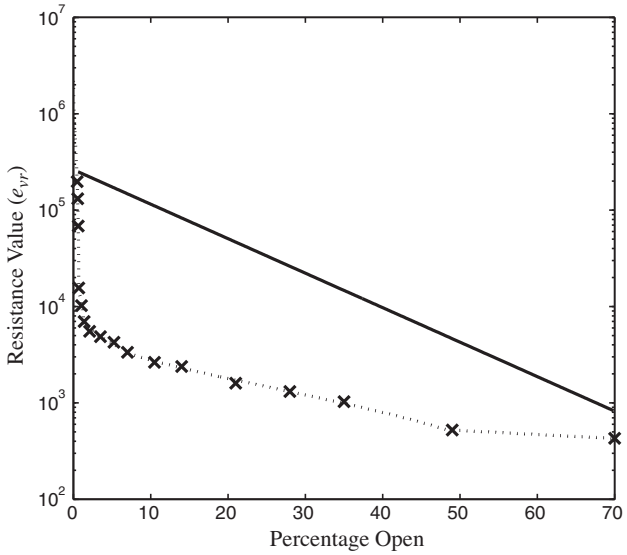


**Fig. 2.** Correlation between valve resistance value ($e_{vr}$) and valve percentage open ($O_p$): commercial data (solid line), experimentally measured data (×), and curve fittings to experimental data (dashed lines) using Eq. (8) and Table 2.

## 3. Optimization-based control for specific energy consumption minimization

After the parameters of the system model Eqs. (1)–(4) have been computed from the experimental step-test data [3], the

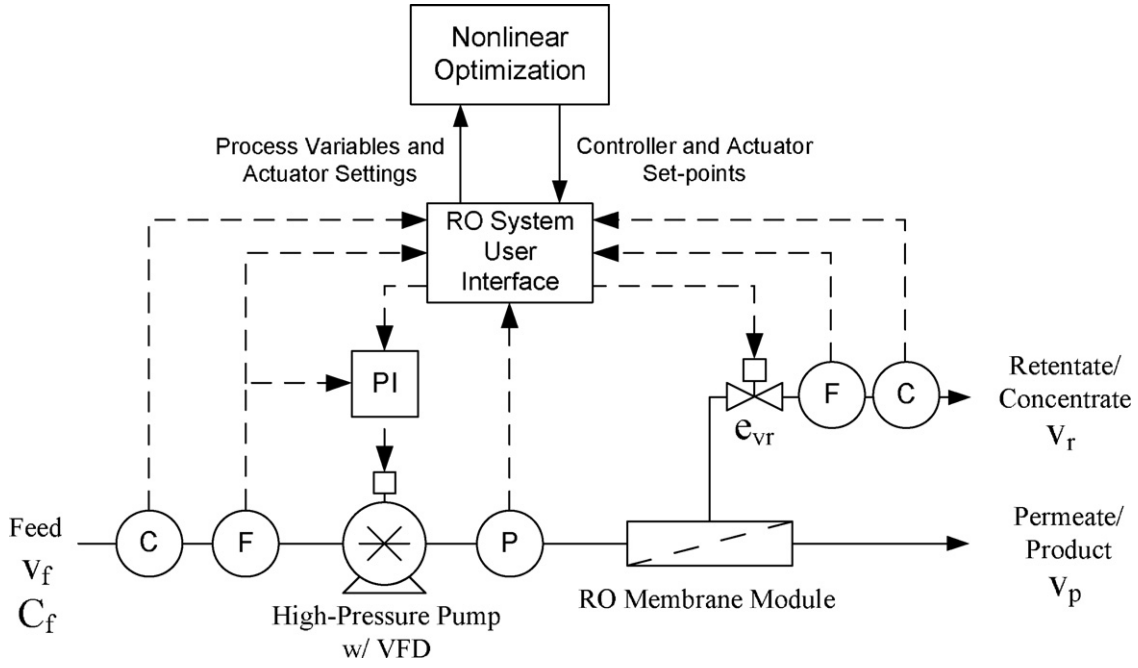


**Fig. 3.** Control diagram detailing data flow between measurement sensors, controllers, actuators, RO system user interface and optimization algorithm.

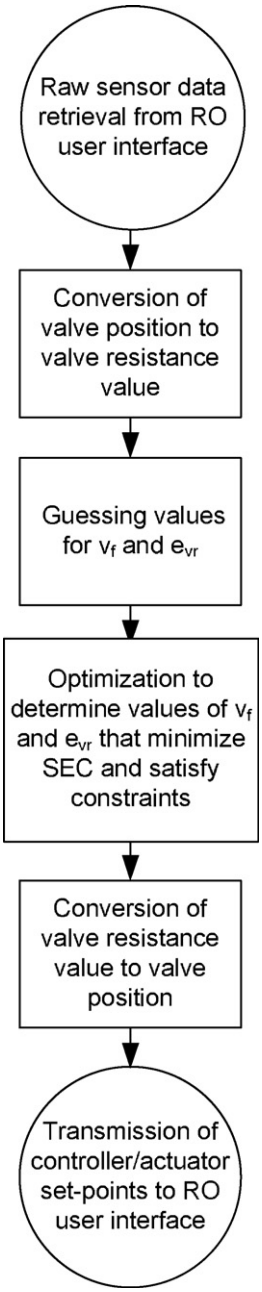


**Fig. 4.** Energy optimization decision process conducted at each sampling time.

energy-optimal controller is designed in order to facilitate system operation at the point of minimum specific energy consumption (for a given rate of water production). Following [3], the experimental system uses data acquisition software to record sensor data in real time. This RO system user interface program is linked with an optimization code (implemented in MATLAB) that performs the energy optimization, which then sends the controller/actuator set-points back to the RO system user interface to be implemented on the system. As seen in Fig. 3, the RO system user interface receives measurements of feed conductivity, feed flow rate, feed pressure, retentate flow rate, and retentate concentration from the process measurement sensors. The optimization code receives the data from the user interface software and carries out the constrained optimization algorithm (see Eq. (15)). When the optimal values for feed flow rate set-point and valve position are determined, these values are passed back to the user interface software and implemented on the system. Since a certain permeate production rate is commonly an operating requirement for RO desalination systems, the optimization algorithm is constrained to finding the optimal control values that satisfy the user-defined permeate production rate set-point. This value for permeate flow rate set-point is user-specified on the system user interface and is also transmitted to the optimization algorithm along with the sensor data.

The objective of the optimization algorithm is to determine the values of feed flow rate ($v_f$) and retentate valve resistance ($e_{vr}$) such that the SEC at the operating condition is minimized and appropriate constraints are satisfied. Substituting Eq. (4) into Eq. (1) and solving for $P_{sys}$, the optimization problem can be represented as:

$$\min_{v_f, e_{vr}} SEC = \min_{v_f, e_{vr}} \frac{\Delta P}{Y} = \min_{v_f, e_{vr}} \frac{\rho e_{vr}(v_f - v_p)^2 v_f}{2v_p} \tag{9}$$

Furthermore, during the optimization, several constraints are imposed; the first of which dictates that a constant permeate production rate is ensured:

$$v_p = v_p^{set} \tag{10}$$

where $v_p^{set}$ is the permeate velocity set-point ($v_p$ is proportional to $Q_p$ through the pipe cross-sectional area, $A_p$). Even though maintaining a specific permeate flow rate will significantly constrain the system, it is necessary because most RO systems are built to address a specific demand for water production. The next constraints ensure that the actuator set-points are positive (negative values have no physical meaning in the experimental system, and the output of negative values may damage the actuators). For the feed flow rate constraint, it is assumed that the feed flow rate is greater than or equal to the permeate flow rate for any reasonable operating condition (no back-flow into the modules through the retentate stream). These constraints dictate that the feed flow rate and the valve resistance (and therefore, the valve position) must be positive.

$$v_f > 0 \tag{11}$$

$$e_{vr} > 0 \tag{12}$$

It is also necessary to constrain the SEC values to be positive in order to achieve the correct optimization variables. This constraint is represented as:

$$SEC \geq 0 \tag{13}$$

Additionally, it is required that the system pressure is greater than the osmotic pressure at the exit of the RO module. If this condition is not satisfied, part of the membrane surface area near the exit region of the module is not utilized to produce permeate water; due to the low applied pressure, the flow across the membrane in this region will actually be reversed (permeate water flowing back into the feed stream). Operation in this region where the transmembrane pressure at the exit region is below the osmotic pressure difference is undesirable, and the process is constrained to operate at or above this limit. This constraint is also called the "thermodynamic restriction" as presented in [21], and has the form:

$$P_{sys} \geq \frac{\pi_0}{1 - Y} \tag{14}$$

In summary, the constrained optimization problem that yields energy-optimal values for the feed flow rate and retentate valve

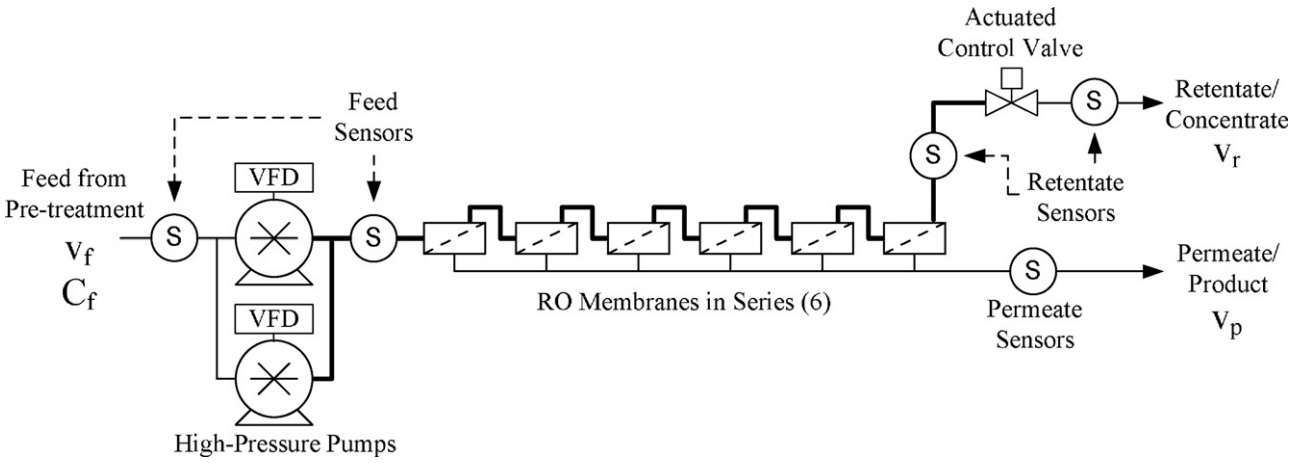


**Fig. 5.** Schematic of RO portion of UCLA's experimental RO membrane desalination system.

resistance can be formulated as follows:

$$\begin{aligned}
&\min_{v_f, e_{vr}} SEC = \min_{v_f, e_{vr}} \frac{\rho e_{vr}(v_f - v_p)^2 v_f}{2v_p} \\
&v_p = v_p^{set} \\
&v_f > 0 \\
&e_{vr} > 0 \\
&SEC \geq 0 \\
&P_{sys} \geq \frac{\pi_0}{1-Y} \\
&0 = \frac{P_{sys}}{\rho} - \frac{1}{2} e_{vr}(v_f - v_p)^2
\end{aligned} \tag{15}$$

On the experimental system, the optimization algorithm conducts multiple steps at every sampling time in order to obtain the control values ($v_f$ and $e_{vr}$) that minimize the SEC for the given permeate flow rate. A detailed flowchart of this process can be found in Fig. 4. First, a UDP (User Datagram Protocol) port is opened to allow for data transmission between the programs. The RO system user interface sends sensor measurements of the feed conductivity, feed flow rate, valve position (converted to valve resistance value as described in Eq. (8)), and permeate flow rate set-point to the optimization algorithm approximately every 10 s. This timestep is dependent on the time taken to conduct the optimization; after the first step, each iteration takes between 1 and 5 s (for the optimization conducted in this work). This timestep can be easily tailored to a different RO system where optimization may take longer due to larger disturbances in the feed or faster changes in system set-points; it may also be allowable to conduct the optimization with lower frequency (depending on the requirements of the system). This repeated real-time optimization is particularly useful in systems where the feed concentration is highly variable or in situations where the target permeate production rate may change over time. After the optimization algorithm receives the raw sensor data and current actuator set-points, the valve position is converted to a valve resistance value (using Eq. (8)) for use along with the current feed flow rate as initial guesses in the sequential quadratic programming (SQP) optimization algorithm (after the first iteration, the previous optimal values are used in order to provide faster convergence). The system model (Eqs. (1)–(4)) is then used to calculate the retentate flow rate, $v_r$, permeate flow rate, $v_p$, system recovery, $Y$, system pressure, $P_{sys}$, and finally the SEC. The calculated variables are checked against the constraints (Eqs. (10)–(14)); if the constraints are not satisfied, the SQP algorithm determines new control values and repeats the process. If the constraints are satisfied, the optimization algorithm determines if the SEC is minimized; if not, the SQP algorithm determines new control values and repeats the process. If the constraints are satisfied and the SEC is minimized, the resulting valve resistance is converted to a valve position and the optimal control values are transmitted to the RO system user interface via the UDP port.

Once the optimization algorithm calculates a feed flow rate set-point and transmits it to the system user interface software, the PI controller uses measurements of the feed flow rate to adjust the variable frequency drive (VFD) in order to achieve the desired feed flow rate set-point. The controller takes the form:

$$VFD_{set} = K_f(Q_f^{sp} - Q_f) + \frac{K_f}{\tau_f}\int_0^t (Q_f^{sp} - Q_f)d\tau \tag{16}$$

where $VFD_{set}$ is the variable frequency drive setting. In this work, $K_f = 0.05$ and $\tau_f = 0.025$. Finally, with the VFD PI controller operating, the RO system user interface applies the actuated valve position retrieved from the optimization code to the actuated retentate valve on the experimental system.

**Remark 1.** Using the UDP data transmission is also advantageous because the computer running the optimization algorithm could be remotely located. This arrangement would allow for centralized energy optimization of multiple RO systems that are spatially distributed, or could allow for a multi-objective optimization formulation that takes into account the production and conditions of multiple RO systems.

## 4. Experimental system description

The experimental reverse osmosis water desalination system constructed at UCLA's Water Technology Research (WaTeR) Center was used for conducting the experiments; please see Fig. 5. This experimental system is comprised of a feed tank, two low-pressure feed pumps in parallel which provide enough pressure to pass the feed water through a series of cartridge filters while also providing sufficient pressure for operation of the high-pressure pumps, two high-pressure pumps in parallel (each capable of delivering approximately 4.3 gal/min at 1000 psi), and a bank of 18 pressure vessels containing Filmtec spiral-wound RO membranes. The high-pressure pumps are outfitted with variable frequency (or variable speed) drives which enable the control system to adjust the feed flow rate by using a 0–10 V output signal. The bank of 18 membranes are arranged into 3 sets of 6 membranes in series; and for the control experiments presented below, only one bank of 6 membrane units was used (in the model, it is assumed that the 6 membranes in series can be represented by one RO module). After

the membrane banks, an actuated valve is used to control the cross-flow velocity ($v_r$) in the membrane units, while also influencing system pressure. The actuated retentate valve and the VFDs are used as actuators for the control system utilizing the control algorithms presented in Section 3. The resulting permeate and retentate streams are currently fed back to the tank in a full-recycle mode, but for field operation the system can be operated in a one-pass fashion.

The experimental system also has an extensive sensor and data acquisition network; flow rates and stream conductivities are available in real-time for the feed stream, retentate stream and permeate stream. The pressures before each high pressure pump, as well as the pressures before and after the membrane units (feed pressure and retentate pressure) are also measured. A centralized data acquisition system takes all of the sensor outputs (0–5 V, 0–10 V, 4–20 mA) and converts them to process variable values on the local (and web-accessible) user interface where the control system is implemented. The data is logged on a local computer as well as on a network database where the data can be accessed via the internet. The data acquisition and control system collects the data at a sampling rate of 10 Hz and implements the actions dictated by the control system on the RO system user interface. More details on the experimental system can be found in [3].

## 5. Results and discussion

In the experiments conducted in this work, the system was initially turned on and the PI controller for feed flow rate was activated. When the system is operated, the permeate and retentate streams are recycled to the feed tank (full-recycle mode). When the system is operated in the full-recycle mode, the feed concentration will not increase over time, since both the permeate and the retentate streams are returned to the feed tank. This concentration increase would only happen if the permeate stream was collected in a separate vessel and only the retentate stream was recycled. Feed solutions with several NaCl concentrations were used (1600 ppm, 1850 ppm, and 3500 ppm) for the experiments presented in this work at pressures ranging from 110 to 170 psi. These operating conditions are typical for the feed salinities presented; however, other brackish water systems (5000–35,000 ppm TDS) and also seawater desalination systems (typically 35,000+ ppm TDS) will operate at higher pressures and usually lower recoveries. After the system reached a steady state, the nonlinear optimization program was activated to begin transmitting the optimal set-point values to the RO system interface. After the set-point values were received by the RO user interface, the set-points were implemented on the actuated retentate valve and the PI controller on the feed pump. The sensor data taken from the experimental system were averaged (before transmission to the optimization code) using a 19 point moving average to remove the majority of the sensor noise. To obtain the other experimental sub-optimal data points (points at higher SEC values), the system was manually adjusted to achieve a range of feed pressures and feed flow rates while maintaining the desired constant permeate flow rate. This process was conducted in order to demonstrate the accuracy of the energy usage model at sub-optimal operating conditions (operating points with higher SEC than the optimal operating point, since the optimization only provides the optimal set-point values for the actuator/controller).

When the system is operating at a fixed permeate flow rate, there exists only one degree of freedom with respect to the operating point. If the feed flow rate is changed, the pressure must take on a specific value to ensure that the permeate flow rate remains constant. The converse is true; if the system pressure is changed, the feed flow rate must take on a specific value in order to maintain the desired permeate flow rate. Because of this, for each normalized permeate flow rate, a single curve exists to describe the specific energy consumption at various recovery values [21].

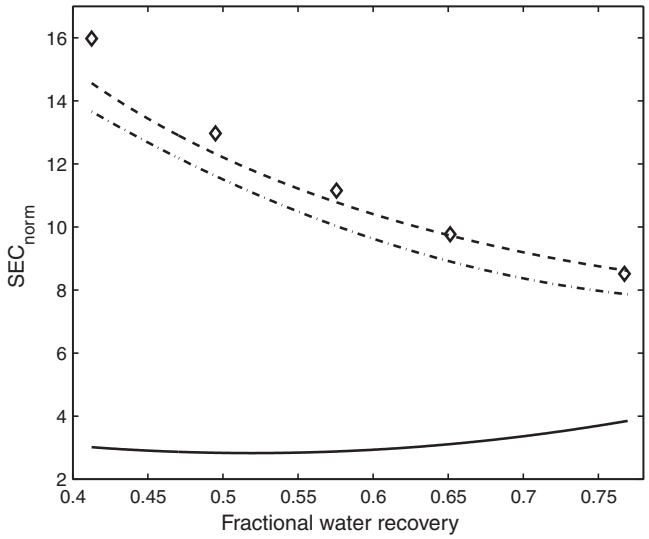


**Fig. 6.** RO system normalized specific energy consumption with respect to fractional water recovery at a fixed permeate flow rate of 1 gpm and a feed salt concentration of 1600 ppm; the dashed line represents the theoretical operating curve assuming 100% salt rejection by the membranes, the dash-dotted line represents the theoretical operating curve accounting for membrane salt rejection, the diamonds represent experimental system data, and the solid line represents the thermodynamic restriction.

The set of experiments presented in Figs. 6–10 demonstrates the experimental system's performance compared to the system performance as predicted by the model for various feed solution salt concentrations. Results for two of the feed solutions (1600 ppm and 1850 ppm) are demonstrated for two different permeate flow rate set-points (1 gpm and 1.45 gpm). In the presentation of the results, the SEC is normalized to $SEC_{norm}$ as discussed in Section 2.

From Figs. 6–10, it can be seen that the experimental system operating points are very close to the theoretically predicted operating points (in terms of specific energy consumption and recovery), for the ideal case of 100% salt rejection by the mem-

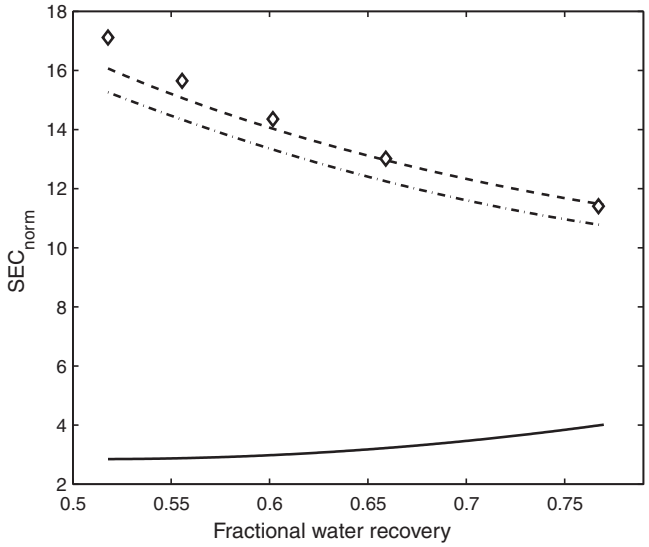


**Fig. 7.** RO system normalized specific energy consumption with respect to fractional water recovery at a fixed permeate flow rate of 1.45 gpm and a feed salt concentration of 1600 ppm; the dashed line represents the theoretical operating curve assuming 100% salt rejection by the membranes, the dash-dotted line represents the theoretical operating curve accounting for membrane salt rejection, the diamonds represent experimental system data, and the solid line represents the thermodynamic restriction.

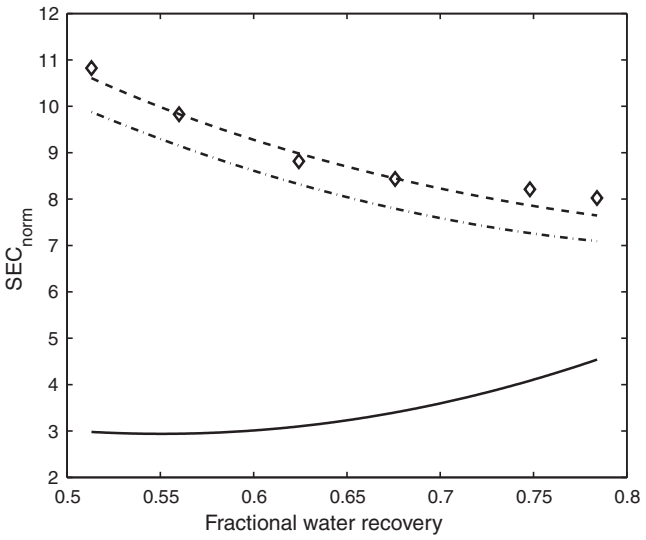


**Fig. 8.** RO system normalized specific energy consumption with respect to fractional water recovery at a fixed permeate flow rate of 1 gpm and a feed salt concentration of 1850 ppm; the dashed line represents the theoretical operating curve assuming 100% salt rejection by the membranes, the dash-dotted line represents the theoretical operating curve accounting for membrane salt rejection, the diamonds represent experimental system data, and the solid line represents the thermodynamic restriction.

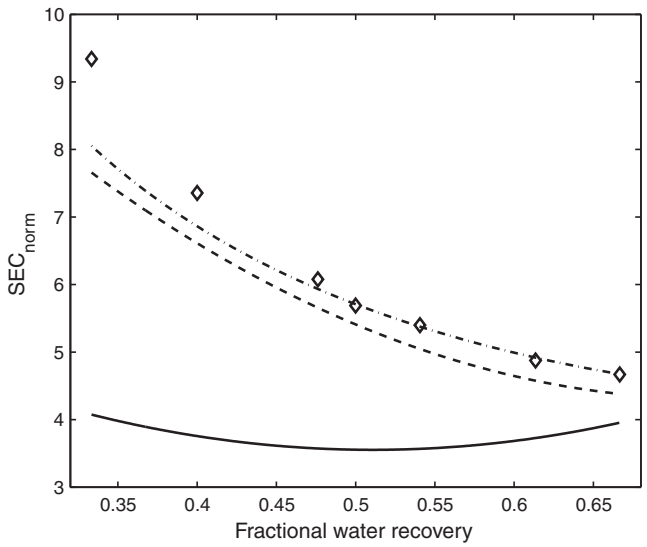


**Fig. 10.** RO system normalized specific energy consumption with respect to fractional water recovery at a fixed permeate flow rate of 1 gpm and a feed salt concentration of 3500 ppm; the dashed line represents the theoretical operating curve assuming 100% salt rejection by the membranes, the dash-dotted line represents the theoretical operating curve accounting for membrane salt rejection, the diamonds represent experimental system data, and the solid line represents the thermodynamic restriction.

branes. It can also be seen that no points are tested at higher recoveries (above the energy optimal operating point dictated by the controller) in order to demonstrate the existence of the minimum specific energy consumption. This is due to the fact that the minimum of the theoretical SEC curve occurs at a point where the physical limitations of the system components prevent experimental system operation at higher recoveries than the optimal one while maintaining the desired permeate flow rate set-point. In Fig. 10, a larger deviation between experimental results and theoretical prediction at lower recovery values can be observed. This is due to the fact that when examining the equation for SEC (Eq. (6)), it can be seen that at low recoveries, experimental errors (sensor noise, etc.) on the recovery value have a larger effect on the calculated SEC value since the recovery appears in the denominator.

Another issue with the theoretical and experimental minimum points is that the resulting permeate salt concentration generally increases with system recovery and can rise above the maximum allowable permeate salt concentration. As mentioned previously in this work, the water produced must maintain a salt concentration below 500 ppm to be consistent with drinking water standards. In Fig. 11, it can be seen that the permeate concentration remains under or near the limit of 500 ppm for the feed solutions with lower salt concentration; however, for the feed solution containing 3500 ppm of NaCl, the permeate salt concentration rises above

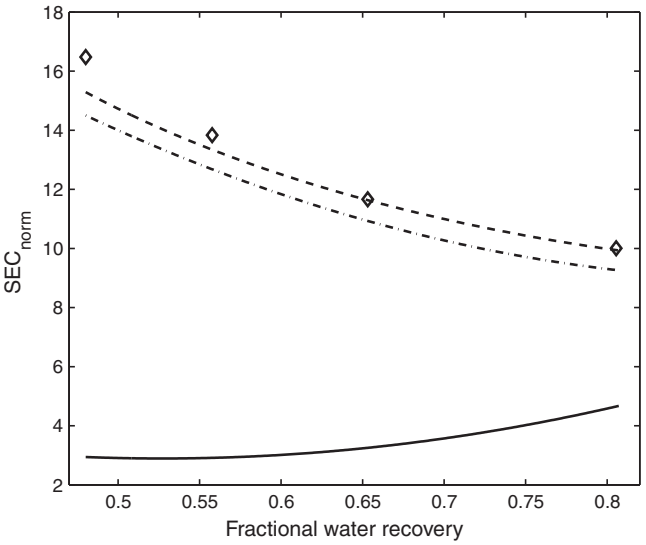


**Fig. 9.** RO system normalized specific energy consumption with respect to fractional water recovery at a fixed permeate flow rate of 1.45 gpm and a feed salt concentration of 1850 ppm; the dashed line represents the theoretical operating curve assuming 100% salt rejection by the membranes, the dash-dotted line represents the theoretical operating curve accounting for membrane salt rejection, the diamonds represent experimental system data, and the solid line represents the thermodynamic restriction.

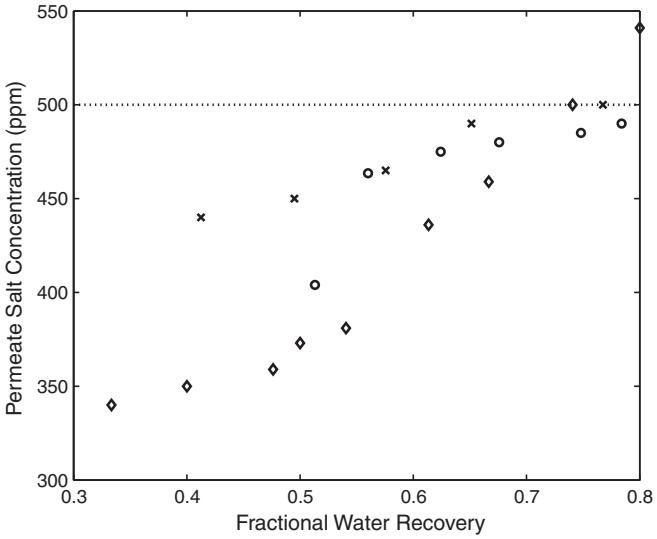


**Fig. 11.** Permeate salt concentration with respect to fractional water recovery at a fixed permeate flow rate of 1 gpm; experimental system data from a feed concentration of 3500 ppm (◊), a feed concentration of 1850 ppm (○), and a feed concentration of 1600 ppm (×). The dotted line represents the permeate salt concentration limit of 500 ppm.

500 ppm for the highest experimental recovery point. This issue arises because the salt rejection (fraction of salt retained on the feed side of the membrane channel) of the membranes is not constant as assumed in the optimization problem in Eq. (15). It has been found that the rejection of the experimental system generally decreases at increasing recovery values (while the constant permeate flow is maintained). It is also found that the membrane salt rejection is not constant at a given water recovery for different feed solution conditions. The salt concentration in the permeate stream increases with increasing recovery, which is observed in the data in Fig. 11.

Since the rejection may be a complex function of the feed flow rate and of the transmembrane pressure, it is very difficult to include this expression in the model as a constraint since its explicit functional form is not available. The rejection is also dependent on (but not limited to) membrane structure, membrane composition, temperature, and the type of ions present in solution. Through these considerations, it can be seen that the rejection will be a complex function of the feed flow rate and of the transmembrane pressure that is unique to each reverse osmosis desalination system. If the rejection can be explicitly described in terms of feed flow rate and transmembrane pressure, then this expression can be used to theoretically determine the permeate concentration at any operating point. An explicit expression for rejection could also be used in the controller formulation as a constraint; in this way, the optimization code could determine the lowest SEC operating point that satisfies the permeate salt concentration standard. In the present work, the membrane rejections for the different water recoveries corresponding to the operating points were determined experimentally and used to re-compute the theoretical operating curve at the user-specified permeate flow rate. The resulting operating curve, accounting for membrane salt rejection, is shown in Figs. 6–10 as the dashed line, and is very close to the experimentally computed operating points.

**Remark 2.** In the most likely situation (as in the current work), the expression for salt rejection dependence on process parameters is not known; therefore, the controller cannot use the rejection (and subsequently, the permeate concentration) as an explicit constraint in the model-based optimization. The simplifications resulting from the lack of knowledge of the salt rejection expression result in the plant-model mismatch observed in the presented data. This mismatch results in the values of the theoretical prediction for the model with complete salt rejection to be, at times, closer to the experimental data collected (although both of the theoretical projections are still equally close to the experimental data within experimental error). Under these circumstances, additional controller operations must be defined in order to "step back" the system operating conditions from the water recovery that gives the optimal SEC to a lower recovery value that provides permeate quality meeting the drinking water standards. It is proposed that the system can institute a procedure where, first, the variable frequency drive speed is increased (this will increase permeate flow rate, ensuring that the total permeate production stays at or above the required value); then, the system will open the retentate valve until the permeate flow rate drops back to the set-point value. In this way, the recovery should be decreased, while the salt rejection should increase, leading to a lower concentration of salt in the permeate stream. A feedback control loop measuring the permeate salt concentration can be used to determine when the permeate quality has reached the desired level; at this point, the "stepping back" procedure can be stopped.

It is also noted that in this work, other important feed water components, such as boron, were not monitored. As these components must be reduced below prescribed limits, it would also be possible (given on-line concentration measurements) to incorporate these limits into the controller formulation presented here as constraints. The resulting controller would be able to use these new measurements along with the existing measurements to ensure that the permeate composition met required standards.

## 6. Conclusions

In this work, an optimization-based control strategy was developed and experimentally implemented on a reverse osmosis (RO) membrane desalination system. First, a non-linear model of the system was derived from first principles and was combined with a model for RO system specific energy consumption to form the basis for the design of an optimization-based control system. The model parameters were computed using experimental system step-test data. The control system uses real-time sensor data and user-defined permeate flow requirements to compute in real-time the energy-optimal set-points for the retentate valve position and feed flow rate. Implementation of the control system on UCLA's experimental RO system demonstrated its ability to achieve energy-optimal operation that is very close to the theoretically predicted energy consumption curves. Future work in this area can include monitoring of other important feed and permeate components (such as boron), investigating scheduled system operation to reduce energy costs based on variations of the electricity price, and accommodating feed/product water storage issues.

## Acknowledgements

Financial support from the State of California Department of Water Resources and the Office of Naval Research is gratefully acknowledged.

## References

[1] A. Rahardianto, J. Gao, C.J. Gabelich, M.D. Williams, Y. Cohen, High recovery membrane desalting of low-salinity brackish water: integration of accelerated precipitation softening with membrane RO, J. Membrane Sci. 289 (2007) 123–137.
[2] I. Alatiqi, H. Ettourney, H. El-Dessouky, Process control in water desalination, Desalination 126 (1999) 15–32.
[3] A.R. Bartman, P.D. Christofides, Y. Cohen, Nonlinear model-based control of an experimental reverse-osmosis water desalination system, Ind. Eng. Chem. Res. 48 (2009) 6126–6136.
[4] C.W. McFall, A.R. Bartman, P.D. Christofides, Y. Cohen, Control and monitoring of a high recovery reverse osmosis desalination process, Ind. Eng. Chem. Res. 47 (2008) 6698–6710.
[5] A. Abbas, Model predictive control of a reverse osmosis desalination unit, Desalination 194 (2006) 268–280.
[6] A.R. Bartman, C.W. McFall, P.D. Christofides, Y. Cohen, Model predictive control of feed flow reversal in a reverse osmosis desalination process, J. Process Control 19 (2009) 433–442.
[7] A. Gambier, E. Badreddin, Application of hybrid modeling and control techniques to desalination plants, Desalination 152 (2002) 175–184.
[8] A. Hossam-Eldin, A.M. El-Nashar, A. Ismaiel, Techno-economic optimization of SWRO desalination using advanced control approaches, Desalination Water Treat. 12 (2009) 389–399.
[9] L. Wurth, R. Hannemann, W. Marquardt, Neighboring-extremal updates for nonlinear model-predictive control and dynamic real-time optimization, J. Process Control 19 (2009) 1277–1288.
[10] S. Skogestad, Plantwide control: the search for the self-optimizing control structure, J. Process Control 10 (2000) 487–507.
[11] M. Krstic, Performance improvement and limitations in extremum seeking control, Syst. Control Lett. 39 (2000) 313–326.
[12] I.M. Alatiqi, A.H. Ghabris, S. Ebrahim, System identification and control of reverse osmosis desalination, Desalination 75 (1989) 119–140.
[13] D. Herold, A. Neskakis, A small PV-driven reverse osmosis desalination plant on the island of Gran Canaria, Desalination 137 (2001) 285–292.
[14] C.C.K. Liu, J. Park, R. Migita, G. Qin, Experiments of a prototype wind-driven reverse osmosis desalination system with feedback control, Desalination 150 (2002) 277–287.
[15] T. Manth, M. Gabor, E. Oklejas, Minimizing RO energy consumption under variable conditions of operation, Desalination 157 (2003) 9–21.
[16] M. Busch, W.E. Mickols, Reducing energy consumption in seawater desalination, Desalination 165 (2004) 299–312.
[17] M. Wilf, C. Bartels, Optimization of seawater RO systems design, Desalination 173 (2005) 1–12.

[18] M. Wilf, Design consequences of recent improvements in membrane performance, Desalination 113 (1997) 157–163.
[19] A. Zhu, P.D. Christofides, Y. Cohen, On RO membrane and energy costs and associated incentives for future enhancements of membrane permeability, J. Membrane Sci. 344 (2009) 1–5.
[20] W.G.J. van der Meer, J.C. van Dijk, Theoretical optimization of spiral-wound and capillary nanofiltration modules, Desalination 113 (1997) 129–146.
[21] A. Zhu, P.D. Christofides, Y. Cohen, Effect of thermodynamic restriction on energy cost optimization of RO membrane water desalination, Ind. Eng. Chem. Res. 48 (2009) 6010–6021.
[22] A. Zhu, P.D. Christofides, Y. Cohen, Minimization of energy consumption for a two-pass membrane desalination: effect of energy recovery, membrane rejection and retentate recycling, J. Membrane Sci. 339 (2009) 126–137.
[23] A. Zhu, A. Rahardianto, P.D. Christofides, Y. Cohen, Reverse osmosis desalination with high permeability membranes – cost optimization and research needs, Desalination Water Treat. 15 (2010) 256–266.
[24] A. Zhu, P.D. Christofides, Y. Cohen, Energy consumption optimization of reverse osmosis membrane water desalination subject to feed salinity fluctuation, Ind. Eng. Chem. Res. 48 (2009) 9581–9589.